JOURNAL OF GEOPHYSICAL RESEARCH, VOL. 88, NO. C5, PAGES 2813–2818, MARCH 30, 1983

# A Mechanism for the Formation of Ice Edge Bands

PETER WADHAMS

*Scott Polar Research Institute, University of Cambridge, Cambridge CB2 IER England*

We propose a mechanism for the formation of multiple bands at an ice edge that is subjected to an off-ice wind. The wind moves the outermost floes seaward faster than the interior ice, dilating the marginal ice zone and opening up random polynyas. In the largest of the polynyas, the off-ice wind generates a significant fetch-limited wave spectrum, which produces a wave radiation pressure on floes at the downwind end of the polynya, increasing their velocity. They are herded against their downwind neighbors, creating a band of high ice concentration. The band is stabilized by an internal compacting stress due to the exponential decay of the wind-wave spectrum across the band and to a slower decay of swell incident from seaward. The band's growth terminates when it encounters a second downwind polynya of sufficiently large size. We show how an array of 'immature' bands generated in this way 'matures' by selective mergers into larger, regularly spaced bands of approximately equal width.

## 1. INTRODUCTION

When an off-ice wind begins to blow across an ice margin composed of small floes, the outermost few kilometres of the icefield often break up into an apparently regular series of ice bands. The bands are typically 1 km wide, 10 km long, are separated by a few kilometers of open water, and lie with their long axes at 40°–90° to the left of the wind direction [*Muench and Charnell*, 1977]. The phenomenon is especially common in the Bering Sea in winter [*Bauer and Martin*, 1980; *Martin et al.*, this issue], although bands of similar dimensions have been observed in the Gulf of St. Lawrence [*Campbell et al.*, 1977, Figure 5], the Antarctic, and the Greenland and Labrador seas. At the Bering Sea ice edge, the outermost band moves seaward faster than its neighbors and quickly melts in the warmer surface water that it encounters. The stripping of ice from the ice edge in bands is therefore a mechanism for a more rapid ablation of the ice margin than would otherwise occur. Figure 1 (by courtesy of S. Martin, University of Washington) shows aerial photographs of Bering Sea ice bands possessing typical characteristics.

In this paper we propose a mechanism for the formation and consolidation of multiple ice bands in which a crucial role is played by the wave radiation pressure of the fetch-limited sea produced by the off-ice wind blowing over an initially random array of water openings (polynyas). This pressure is concentrated on the floes at the immediate downwind end of each polynya and herds them against their neighbors further downwind. Once a band forms, the exponential decay of the wind sea across it generates an internal compacting stress, which helps to maintain the band's integrity, an effect enhanced by the swell incident on the band from seaward.

## 2. MAGNITUDE OF THE FORCES ACTING ON FLOES

A case study discussed by *Bauer and Martin* [1980] enables us to assess the relative magnitude of the forces causing band generation and movement. During a 14-hour period, they observed a band move at an average speed of 0.4 m s$^{-1}$ at 25° to the right of an off-ice wind of 10 m s$^{-1}$. The band's long axis lay at right angles to the wind. The remainder of the pack moved at only 0.15 m s$^{-1}$ in the same direction, so the band separated itself from the pack and moved approximately 20 km out into the open water zone before rapidly deteriorating.

The major forces on the floes are assumed to be aerodynamic wind drag, hydrodynamic water drag, and wave radiation pressure. Tidal and inertial forces, while important, are presumed to affect the shape, orientation, and trajectory of the band rather than accounting for its existence as such. The total wind drag $\mathbf{F}_a$ on a floe is

$$\mathbf{F}_a = \rho_a C_a A |\mathbf{U}_a - \mathbf{U}_i| (\mathbf{U}_a - \mathbf{U}_i) \tag{1}$$

and the water drag $\mathbf{F}_w$ is

$$\mathbf{F}_w = -\rho_w C_w A |\mathbf{U}_i - \mathbf{U}_w| (\mathbf{U}_i - \mathbf{U}_w) \tag{2}$$

where $\rho$ is density, $C$ is a drag coefficient, $A$ is surface area $U$ is velocity, and $a$, $i$, $w$ denote air, ice, and water, respectively.

Bauer and Martin, following *Squire and Moore* [1980], showed that swell incident on the Bering Sea ice edge from the open sea breaks up the ice through flexural failure and rafts the outermost floes so that typically the resulting ice marginal region consists of three zones: (1) an edge zone 5–10 km wide, consisting of small, extensively rafted floes typically 20 m in diameter and 2–4 m thick; (2) a transition zone about 5 km wide consisting again of small (20 m) floes with rafting to only 0.3–0.6 m thickness; and (3) an interior zone consisting of large ($\sim$1 km) unrafted floes 0.2–0.3 m thick. $C_a$ and $C_w$ will be different in each of these zones. The equilibrium drift velocity $U_i$ for a floe under wind forcing and water drag is given by equations (1) and (2) as, neglecting $U_w$,

$$U_i^2 = U_a^2 \frac{\rho_a C_a}{\rho_w C_w} \tag{3}$$

and therefore can be expected to vary from zone to zone. Little direct experimental data on $C_a$ and $C_w$, however, exist for the marginal ice zone (MIZ). The only measurement of $C_a$ was by *Smith et al.* [1970], who found a value of $3.1 \times 10^{-3}$ in a pack composed of small broken floes in the Gulf of St. Lawrence, compared with typical values of $1.4$–$2.1 \times 10^{-3}$ over a continuous ice cover [*Banke et al.*, 1976, 1980]. No measurement of $C_w$ has been made in the marginal ice zone, and values from the central Arctic lie in the range $3.4 \times 10^{-3}$ [*McPhee and Smith*, 1975] in winter to $5.5 \times 10^{-3}$ in summer [*McPhee*, 1980]. The MIZ differs from the central Arctic in possessing an ice cover of discrete floes at less than 100% concentration. This implies that a mature oceanic boundary layer is unlikely to exist; also, the



Paper number 2C1113.
0148-0227/83/002C-1113$05.00

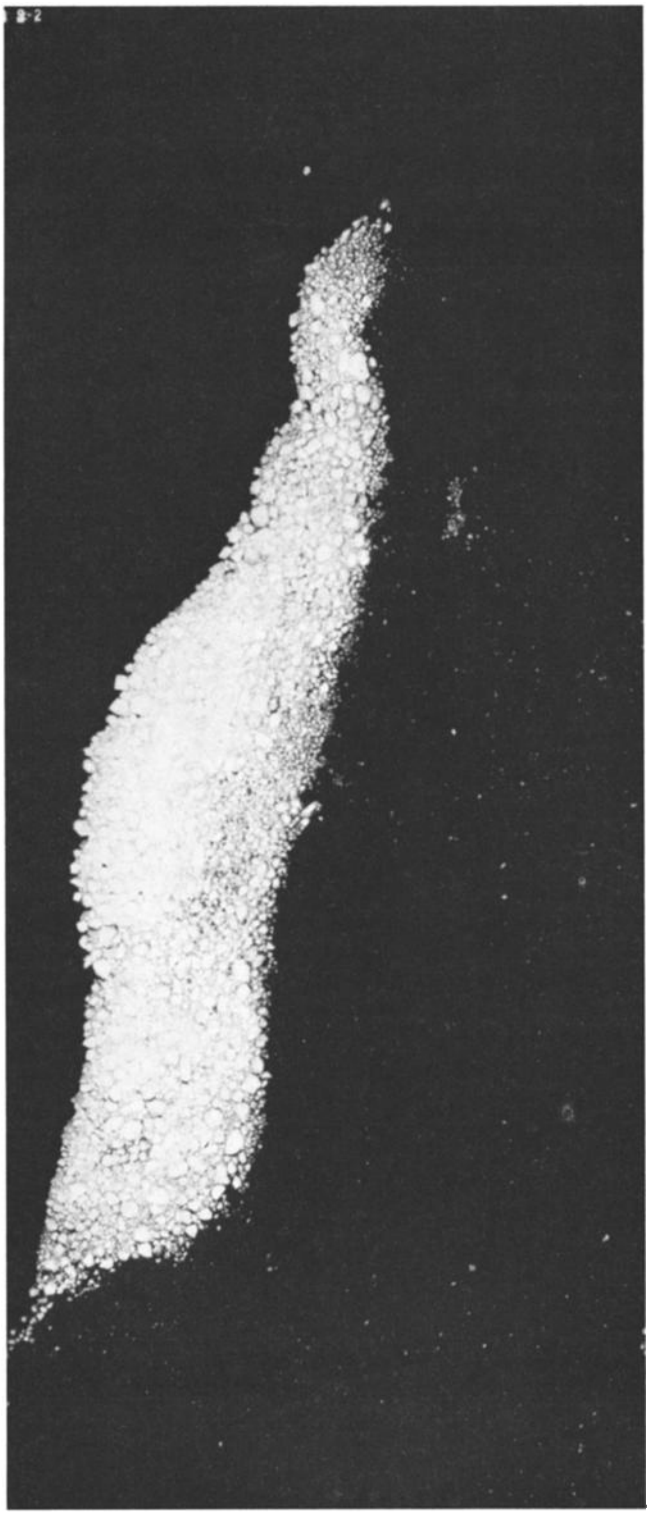

Fig. 1*a*

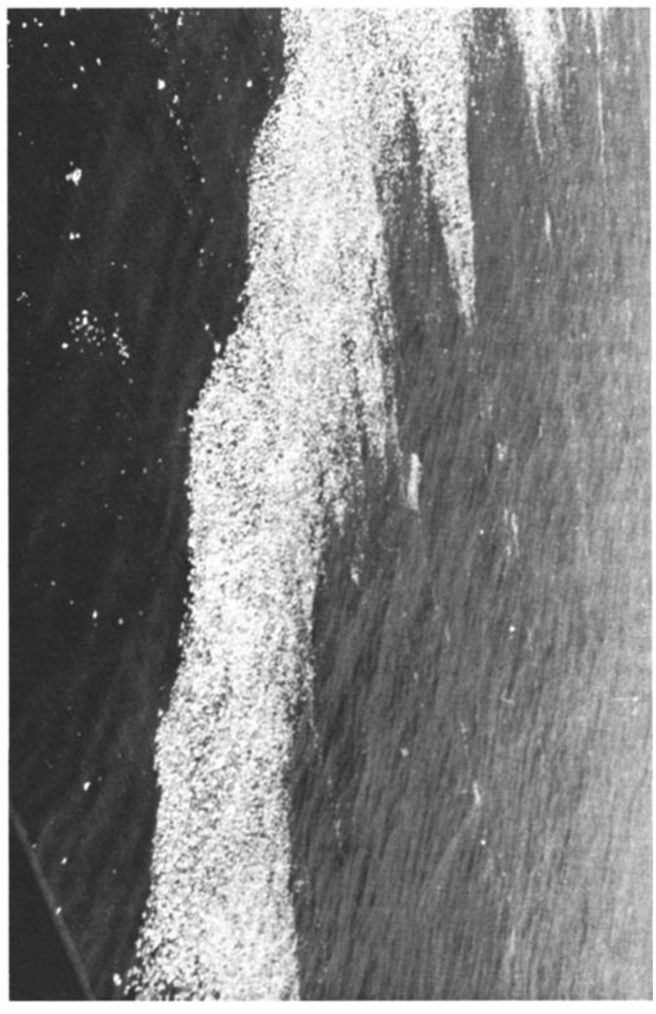

Fig. 1*b*

Fig. 1. Bering Sea ice bands, March 1979. (*a*) A band of length 525 m, maximum width 100 m, composed of floes of 10 m diameter. *N* is at top of photo, wind is from NE, 7 m $s^{-1}$. (*b*) Part of a band of small (1-2 m) ice cakes, showing wind sea (wind 9 m $s^{-1}$) on iceward side and swell on seaward side.

absence of deep pressure ridges tends to reduce $C_w$, but this is more than offset by the contribution of form drag due to floe edges. The resulting $C_w$ is probably greater than in the central Arctic, but not so great as to reduce the $C_a/C_w$ ratio, since the experimental observation of Bauer and Martin was that as soon as an off-ice wind began to blow, the edge zone floes moved seaward faster than the transition zone which in turn moved faster than the interior ice (i.e., there was an overall dilation of the MIZ giving a reduced ice concentration dispersed as an initially random distribution of floes).

It is the edge zone floes that participate in band formation; and if we use the above value of $3.1 \times 10^{-3}$ for $C_a$, a guessed value of $7 \times 10^{-3}$ for $C_w$, $U_a = 10$ m s$^{-1}$, $U_i = 0.4$ m s$^{-1}$ ($U_w$ assumed zero), and $A = 400$ $m^2$ (a 20 m diameter floe), we obtain for Bauer and Martin's case study,

$$F_a = 162 \text{ N}$$

$$F_w = 460 \text{ N}$$

Therefore, the wind stress alone is unable to drive the floes at the observed speed, and we must turn to the third element, wave radiation pressure.

*Longuet-Higgins* [1977] showed that when a wave is incident on a floating body, the force on the body per unit width of wavefront is, in deep water,

$$F_r = \tfrac{1}{4}\rho_w g(a^2 + a'^2 - b^2) \tag{4}$$

where $a$, $a'$, $b$ are amplitudes of the incident, reflected, and transmitted waves, respectively. The force is exerted in the direction of propagation of the wave. *Wadhams* [1973, 1975, 1978, 1983] developed the theory of the reflection and transmission of waves by ice floes and found good agreement with field observations from submarine sonars, airborne lasers, and wave buoys. The reflection coefficient ($a'/a$) is large for short period waves and approaches unity when the floe diameter exceeds half a wavelength. We also expect an effect of draft on reflection, with the submerged walls of the floe acting as a vertical barrier to short waves; this gives a large reflection coefficient if the floe draft exceeds half a wavelength [*Ursell*, 1947]. Such short period waves (less than 2–4 s period) are not dominant in an open-ocean spectrum, but they do dominate the fetch-limited spectrum that occurs when wind blows across a short expanse of open water of the size that could open at random within a dilating MIZ.

Assuming zero absorption, (4) simplifies to

$$F_r = \tfrac{1}{2}\rho_w g a^2 R^2 \tag{5}$$

where $R = a'/a$ is the amplitude reflection coefficient. The force on a floe is $F_r d$ where $d$ is the diameter, and for a 20 m floe with $R = 1$ the wave force is 1000 $N$ for $a = 0.1$ m. This clearly outweighs $F_a$ and is sufficient to match $F_w$ and thus propel the floes in the band at the observed speed.

## 3. DESCRIPTION OF THE MODEL

A qualitative description of the band formation model is as follows.

*First stage.* In initially wind-free conditions, incident long waves and swell from the open sea (including swell from the Pacific coming through gaps between the Aleutians) work upon the MIZ to produce zones of differing ice morphology, the smallest floes being found in the outermost zone. The mechanism of floe breakup by wave-induced failure is described by *Goodman et al.* [1980].

*Second stage.* When an off-ice wind begins to blow (and winds from this sector are typical of winter in the Bering Sea [*Pease*, 1980]) the edge zone floes are blown seaward slightly faster than the interior ice, and so a general dilation of the MIZ occurs. This opens polynyas of random sizes and orientations within the pack. The process is illustrated in Figure 2, which shows computer simulations of a 1 km × 1 km icefield composed of a random array of 20 m floes in 50 and 25% concentrations. Even in the 50% icefield, there is a polynya of 200 m downwind fetch, while the 25% icefield contains several large polynyas of 240 m downwind and crosswind dimensions.

Fig. 2 (top)

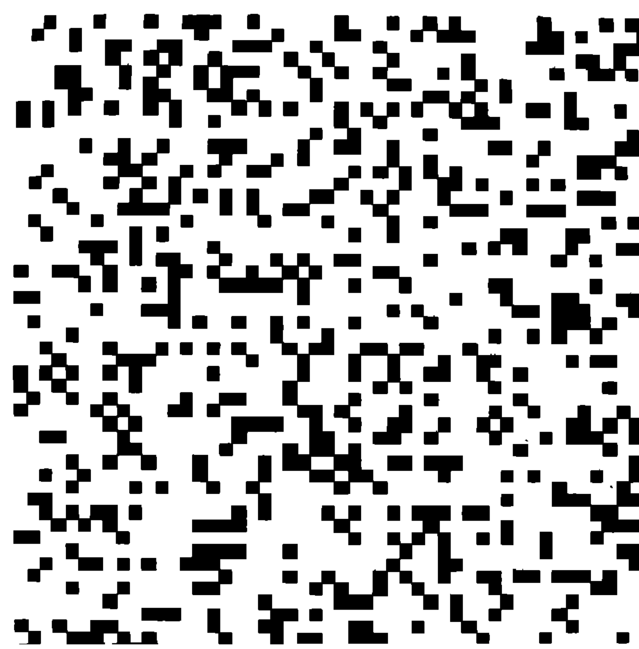

Fig. 2 (bottom)

Fig. 2. Random 1 km × 1 km arrays of 20 m-square floes in (top) 50% and (bottom) 25% concentration. Ice is black.

*Third stage.* In the largest of these randomly created openings, the off-ice wind generates a significant fetch-limited spectrum of steep short-period waves. These exert a radiation pressure on floes at the downwind end of the polynya; the pressure is significant because of the almost total reflection that occurs. The pressure increases the downwind speed of the floes. This in turn increases the size of the polynya, increases the fetch, in-

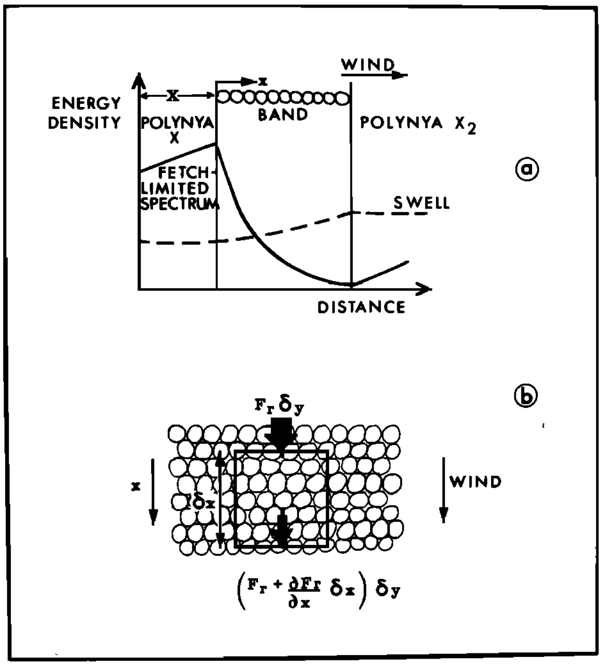


Fig. 3. (*a*) Schematic diagram of exponential decays of fetch-limited wave energy and swell energy across a band. (*b*) Wave radiation forces on two sides of an area $\delta x\ \delta y$ in the band interior, illustrating origin of compacting force.

creases the wave energy at the downwind end, and still further increases the radiation pressure. As the floes at the downwind end of the growing polynya catch up on floes further downwind shielded from the wave energy, they sweep them into a compact band of high ice concentration. The downwind orientation of the forcing causes the bands to have a long axis lying crosswind; this process may be assisted by a tendency for the initial polynyas to have long axes lying crosswind, owing to surface currents caused by internal waves [*Muench et al.*, this issue].

*Fourth stage.* Once established, the band keeps its integrity because of the wave force on its upwind side. In addition, once the fetch has increased to the point where longer waves are generated that give $R < 1$, the radiation pressure begins to exert a compressive force throughout the width of the band. This is reinforced by a similar, though weaker, compressive force due to swell incident from seaward. The mechanism is again that of partial wave energy reflection from each floe [*Wadhams*, 1973, 1975]. Each layer of floes that the wavefront encounters causes partial reflection, and the progressive partial reflection is equivalent to an exponential decay of the forward-going wave energy with distance. An initial amplitude $a_0$ is reduced to $a_x$ in a distance $x$ such that

$$a_x = a_0 \exp(-\alpha x) \tag{6}$$

where $\alpha$, the amplitude attenuation coefficient, is is given by [*Wadhams*, 1973]

$$\alpha = \frac{pR^2}{2d} \qquad (R < 1) \tag{7}$$

Here $p$ is the fraction of the sea surface occupied by ice. Thus a wave radiation force $\mathbf{F}_r$ per unit wavefront is perceived within the band as a compressive force of $(-d\mathbf{F}_r/dx)$ per unit wavefront acting on every element of the icefield (Figure 3). Its magnitude is

$$-\frac{dF_r}{dx} = \rho_w g R^2 {a_x}^2 \alpha = \frac{\rho_w g p R^4 {a_x}^2}{2d} \tag{8}$$

For $R = 0.5$, $p = 1$, $d = 20$ m, $a_x = 0.1$ m, the compressive force is 0.2 N m$^{-1}$, which helps to maintain the integrity of the band, especially near the windward end where $a_x$ is greatest. In a similar way, the compressive force due to the radiation pressure of swell is greatest near the leeward (i.e., seaward) end of the band; its magnitude will be less because the low value of $R$ at long wave periods (about 0.3 at 8 s, 0.1 at 12 s for a 20 m floe [*Wadhams*, 1973, 1983]) more than offsets the higher amplitude of the swell.

In summary then, the dominant forces are (1) force originating band: off-ice wind drag on rough 'edge zone' floes, making them move seaward slightly faster than remainder of pack, which dilates the MIZ and opens random polynyas; (2) force consolidating band: radiation pressure on floes at downwind ends of larger polynyas due to fetch-limited wind-wave spectrum generated in the polynya; (3) forces maintaining band: compressive forces due to exponential decay of fetch-limited wave spectrum passing into band from windward, and swell spectrum passing into band from leeward (seaward); and (4) forces separating band from pack: fetch-limited wave radiation pressure plus excess wind drag minus swell radiation pressure.

## 4. Some Quantitative Estimates

If a 50 km × 100 km area of MIZ composed of 20 m floes is dilated to 50% concentration as shown in Figure 2, we expect statistically to find one polynya with a downwind fetch of 460 m. Taking 400 m, then, as a conservative size for a large random polynya and $U_a = 10$ m s$^{-1}$ as the wind speed, we can estimate the fetch-limited wave spectrum at the downwind end

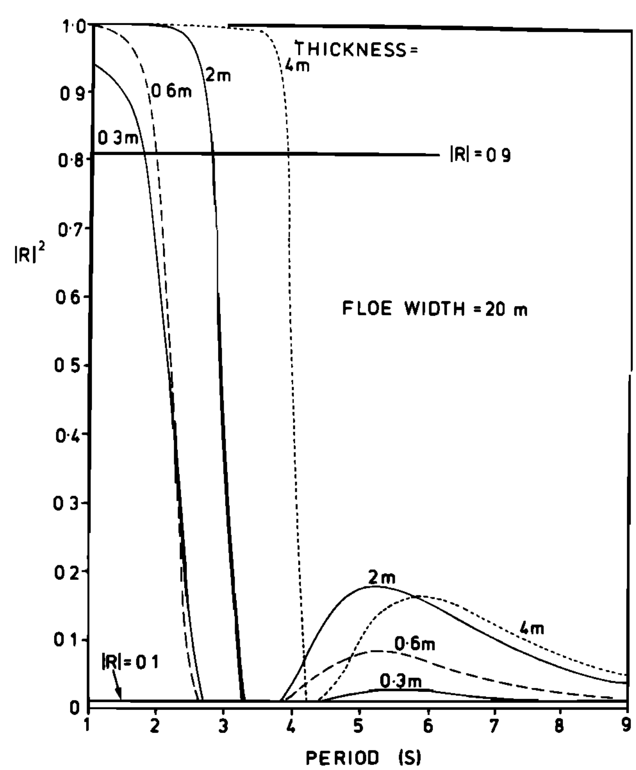


Fig. 4. Energy reflection coefficient $|R|^2$ of floes of width 20 m and thickness 0.3–4 m to waves of period 1–9 s. The curves are cut off below $|R| = 0.1$.

from one of the empirical formulae proposed by *Wu* [1969], *Hasselmann et al.* [1973] or *Phillips* [1977]. They give the dominant radian frequency $\omega_0$ in the spectrum as a function of fetch $X$ as follows:

Wu

$$\omega_0 = 20.0\left[\frac{g^7}{X^3 U_a^4}\right]^{1/10} \tag{9}$$

Hasselmann et al.

$$\omega_0 = 22.0\left[\frac{g^2}{X U_a}\right]^{1/3} \tag{10}$$

Phillips

$$\omega_0 = 2.2\left[\frac{g^3}{X U_*^2}\right]^{1/4} \tag{11}$$

(9) and (10) agree in predicting a dominant period of 1.0 s; (11) gives a somewhat longer period, depending on what we take for the friction velocity $U_*$ (Phillips recommends $U_a = 20\ U_*$). Phillips predicts the mean square surface displacement $\overline{\xi^2}$ to be

$$\overline{\xi^2} = 1.6 \times 10^{-4} X U_*^2/g \tag{12}$$

Again, taking $U_a = 20\ U_*$, this gives $\xi_{rms} = 0.04$ m. If we approximate the whole spectrum by a single sinusoidal wave of the dominant period 1.0 s, then it will have an amplitude of $\sqrt{2}\xi_{rms} = 0.057$ m.

Figure 4 shows the result of applying *Wadhams'* [1973, 1983] theory to calculate the reflection coefficient of floes of 20 m diameter and thickness varying from 0.3 to 4 m. At 1 s period, $R$ is nearly unity for all thicknesses. To obtain an $R$ of less than 0.9 requires periods of 1.5 s at 0.3 m thickness, 2 s at 0.6 m, and 2.8 s at 2 m, corresponding to fetches of 1.5 km, 4 km, and 12 km, respectively. Thus, during the time of initial formation, before the band moves far from its neighbors, almost all of the wave energy is reflected from the first row of floes in the band. The wave force is therefore exerted almost entirely on the upwind face of the band, and the interior compressive force is negligible.

Using the same drag coefficients as in section 2, we again obtain $F_a = 162$ N as the wind drag on a single 20 m floe, but the water drag is now

$$F_w = 2870 U_i^2 \tag{13}$$

We neglect $U_w$ in calculating $F_w$, and $U_i$ in calculating $F_a$. The balance of $F_a$ and $F_w$ gives us the floe velocity, $U_0$, say which occurs in the absence of wave forcing and which can be taken as the downwind velocity of the pack as a whole. Here, $U_0 = (162/2870)^{1/2} = 0.24$ m s$^{-1}$. With wave radiation pressure added, the force balance becomes

$$F_a + F_r d = F_w \tag{14}$$

Using (5) for $F_r$, with $R = 1$ and a calculated from (12), we obtain

$$F_r d = 0.82X \text{ N} \tag{15}$$

With $X = 400$ m as the initial fetch, we obtain $U_i = 0.41$ m s$^{-1}$ from (14). A floe at the downwind end of the initial polynya therefore moves 0.17 m s$^{-1}$ faster than a floe sheltered from the wave field. The polynya begins to widen at 10 m per minute, and the downwind floes soon begin to 'sweep up' their nearest downwind neighbors.

As soon as this happens, however, the 'protoband' thus

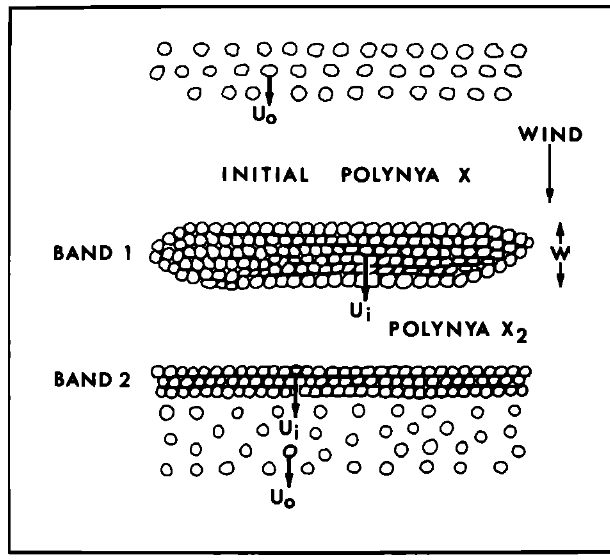


Fig. 5. Schematic diagram of a band that has reached its terminal width $W$ and is now moving as fast as floes at the downwind end of polynya $X_2 (X_2 < X)$ which are just beginning to form a second band.

formed begins to slow down. Consider a band that has acquired an average width of $n$ floes (Figure 5). Each floe is still subject to the same air and water stress as before, neglecting variations in form drag due to the floes being bunched together. However, the wave force is exerted only on the first row of floes, so its effect is diluted as the band grows wider. For the band as a whole, (13) and (14) give

$$U_i^2 = U_0^2 + \frac{0.82X}{2870n} \tag{16}$$

so that $U_i$ drops toward $U_0$ as $n$ increases, although partially offset by the growth in $X$. Eventually, the band attains a width such that it can no longer continue to sweep up floes—it will catch up with a second random polynya, which may be smaller than the first (Figure 5) but still be large enough to give its own downwind floes enough additional speed to keep ahead of the band. The band has now reached its maximum size, and the downwind polynya that halts its growth becomes the seed polynya for the next band. Thus we now have a mechanism for multiple bands.

If we assume that during its growth phase the band sweeps up floes uniformly spaced within a fractional cover $p$, and that it then encounters a stopping polynya of width $X_2$, we can generalize (16) to give the final width $W$ of the band as

$$W = d\left[\frac{Xp - d(1-p)}{X_2 p - d(1-p)}\right] \tag{17}$$

and the final width of the generating polynya as

$$X(\text{final}) = X + \frac{(W-d)(1-p)}{p} \tag{18}$$

(17) is obtained by balancing the final band speed against the floe speed downwind of $X_2$. Using our standard values for $d$ and $X$, and assuming the stopping polynya to be 100 m wide, these equations give a final band width of 95 m in a 50% icefield and 170 m in a 25% icefield. The corresponding final widths of the generating polynya are 480 m and 850 m, respectively, which may be taken as the spacing between bands.

## 5. Multiple Bands

The formation of multiple bands is thus straighforward to visualize (Figure 5). Band 1 is produced by a given starting polynya $X$, which represents an extremum of a random distribution of floe spacings caused by wind-induced icefield dilation. Band 1 begins by rapidly sweeping up floes, causing $X$ to increase slowly but the band speed $U_i$ to decrease quickly toward $U_0$, the speed of an isolated sheltered floe, as the width of the band increases. Eventually, the band slows to the point where, as soon as the sweeping-up operation comes across a second polynya $X_2$ of more modest size, the band cannot catch up with the floes at the downwind end of $X_2$ which are themselves subject to a wave pressure from the fetch $X_2$. $X_2$ can now form the starting point of a second downwind band, band 2. And so on.

In this way, the whole MIZ region organizes itself into bands from an initially random array of floes. The bands thus formed, which may be termed 'immature bands,' will be of varying width and varying spacing, since (17) and (18) show that band growth terminates at a point dependent on a random encounter with a second polynya $X_2$, of sufficient size (there is no upper limit on $X_2$, while the lower limit is given by (17)). This first organizing process, however, is then followed by a maturing process by which the band distribution evolves toward uniformity of width and spacing. This is because immature bands will tend to merge according to two laws:

*Law 1.* Other things being equal, a wide band moves more slowly than a narrow band, so narrow bands will catch up with wide bands and merge with them.

*Law 2.* Other things being equal, a band with a small upwind fetch moves more slowly than a band with a large upwind fetch, so bands driven by large fetches will catch up with bands driven by small fetches and merge with them.

The result will be a small number of 'mature bands' that are wider and spaced further apart than the initial bands analyzed in section 4, with the widths and spacings tending toward regularity.

## 5. Conclusions

For simplicity we have ignored a number of important forces, such as Coriolis force, which will give the floes a trajectory with a mean vector to the right of the wind, ocean tilt, tidal currents, and wind-induced drift currents [*Wu*, 1975], which lead to an overall downwind streaming of the ice and surface water. Nevertheless, we believe that we have demonstrated a mechanism by which surface waves, acting on the random openings of a diffuse icefield, can organize such an icefield into a series of equally wide and equally spaced bands under an off-ice wind.

*Acknowledgments.* I acknowledge with thanks the effect of many useful discussions with Seelye Martin, Jane Bauer, and Vernon Squire. I thank Rob Massom for diagrams and Ruth Weintraub and Steve Lamont for computing. Figure 1 is due to S. Lyn McNutt and Seelye Martin, and was taken from a C-130 of NASA Johnson Space Center. This paper is dedicated to Maria Elizabeth Coryell-Martin, born on the completion date.

## References

Banke, E. G., S. D. Smith, and R. J. Anderson, Recent measurements of wind stress on Arctic sea ice, *J. Fish. Res. Bd., Canada, 33*, 2307–2317, 1976.

Banke, E. G., S. D. Smith, and R. J. Anderson, Drag coefficients at AIDJEX from sonic anemometer measurements, in *Sea Ice Processes and Models*, edited by R. S. Pritchard, pp. 430–442, University of Washington Press, Seattle, 1980.

Bauer, J., and S. Martin, Field observations of the Bering Sea ice edge properties during March 1979, *Mon. Weather Rev., 108*, 2045–2056, 1980.

Campbell, W. J., R. O. Ramseier, R. J. Weaver, and W. F. Weeks, Skylab floating ice experiment, *Misc. Spec. Publ. 34*, Dept. of Fisheries and the Environ., Fish. and Mar. Serv., Ottawa, Canada, 1977.

Goodman, D. J., P. Wadhams, and V. A. Squire, The flexural response of a tabular ice island to ocean swell, *Ann. Glaciol., 1*, 23–28, 1980.

Hasselmann, K., et al., Measurements of wind wave growth and swell decay during the Joint North Sea Wave Project (JONSWAP), *Herausgegeben Deutsch. Hydro. Institut.*, Reihe A, 1973.

Longuet-Higgins, M. S., The mean forces exerted by waves on floating or submerged bodies with applications to sand bars and wave power machines, *Proc. R. Soc., London, Ser. A, 352*, 463–480, 1977.

McPhee, M. G., An analysis of pack ice drift in summer, in *Sea Ice Processes and Models*, edited by R. S. Pritchard, pp. 62–75, University of Washington Press, Seattle, 1980.

McPhee, M. G., and J. D. Smith, Measurements of the turbulent boundary under pack ice, *AIDJEX Bull., 29*, 49–92, 1975.

Martin, S., P. Kauffman, and C. Parkinson, The movement and decay of ice edge bands in the winter Bering Sea, *J. Geophys. Res.*, this issue.

Muench, R. D., and R. L. Charnell, Observations of medium-scale features along the seasonal ice edge in the Bering Sea, *J. Phys. Oceanogr., 7*, 602–606, 1977.

Muench, R. D., P. H. LeBlond, and L. E. Hachmeister, On some possible interactions between internal waves and sea ice in the marginal ice zone, *J. Geophys. Res.*, this issue.

Pease, C. H., Eastern Bering Sea ice processes, *Mon. Weather Rev., 108*, 2015–2023, 1980.

Phillips, O. M. *The Dynamics of the Upper Ocean*, 2nd ed., Cambridge University Press, New York, 1977.

Smith, S. D., E. G. Banke, and O. M. Johannessen, Wind stress and turbulence over ice in the Gulf of St. Lawrence, *J. Geophys. Res., 75*, 2803–2812, 1970.

Squire, V. A., and S. C. Moore, Direct measurement of the attenuation of ocean waves by pack ice. *Nature, Lond., 253*, 365–368, 1980.

Ursell, F., The effect of a fixed vertical barrier on surface waves in deep water, *Proc. Cambridge Phil. Soc., 43*, 374–382, 1947.

Wadhams, P., The effect of a sea ice cover on ocean surface waves, Ph.D. thesis, Univ. of Cambridge, 1973.

Wadhams, P., Airborne laser profiling of swell in an open ice field, *J. Geophys. Res., 80*, 4520–4528, 1975.

Wadhams, P., Wave decay in the marginal ice zone measured from a submarine, *Deep Sea Res., 25*, 23–40, 1978.

Wadhams, P., *The Seasonal Ice Zone*, in *NATO Advanced Study Institute on Air-Sea-Ice Interaction*, Plenum, New York, 1983.

Wu, J., Wind stress and surface roughness at air-sea interface, *J. Geophys. Res., 74*, 445–455, 1969.

Wu, J. Wind-induced drift currents, *J. Fluid Mech., 68*, 49–79, 1975.

(Received February 22, 1982;
revised July 20, 1982;
accepted July 20, 1982.)